Eur Radiol (2010) 20: 1374–1383
DOI 10.1007/s00330-009-1679-9

MAGNETIC RESONANCE

Ute Eisenberger
Harriet C. Thoeny
Tobias Binser
Mathias Gugger
Felix J. Frey
Chris Boesch
Peter Vermathen

Evaluation of renal allograft function early after transplantation with diffusion-weighted MR imaging

Received: 28 May 2009
Revised: 31 August 2009
Accepted: 17 September 2009
Published online: 16 December 2009

Ute Eisenberger and Harriet C. Thoeny contributed equally to this work.

U. Eisenberger · F. J. Frey
Department of Nephrology and Hypertension,
University Hospital of Bern,
Bern, Switzerland

H. C. Thoeny
Department of Radiology,
Neuroradiology and Nuclear Medicine,
University Hospital of Bern,
Bern, Switzerland

T. Binser · C. Boesch · P. Vermathen
Department of Clinical Research,
University Hospital of Bern,
Bern, Switzerland

M. Gugger
Department of Pathology,
University Hospital of Bern,
Bern, Switzerland

P. Vermathen (✉)
Department of Clinical Research/
AMSM, University Bern,
Pavillon 52, Inselspital,
P.O. Box 35, 3010 Bern, Switzerland
e-mail: Peter.Vermathen@insel.ch
Tel.: +41-31-6328174
Fax: +41-31-6320580

Abstract *Aims:* To determine the inter-patient variability of apparent diffusion coefficients (ADC) and concurrent micro-circulation contributions from diffusion-weighted MR imaging (DW-MRI) in renal allografts early after transplantation, and to obtain initial information on whether these measures are altered in histologically proven acute allograft rejection (AR). *Methods:* DW-MRI was performed in 15 renal allograft recipients 5–19 days after transplantation. Four patients presented with AR and one with acute tubular necrosis (ATN). Total ADC (ADC_T) was determined, which includes diffusion and micro-circulation contributions. Furthermore, diffusion and micro-circulation contributions were separated, yielding the "perfusion fraction" (F_P), and "perfusion-free" diffusion (ADC_D). *Results:* Diffusion parameters in the ten allografts with stable function early after transplantation demonstrated low variabilities. Values for ADC_T and ADC_D were ($\times 10^{-5}$ mm^2/s) 228±14 and 203±9, respectively, in cortex and 226±16 and 199±9, respectively, in medulla. F_P values were 18±5% in cortex and 19±5% in medulla. F_P values were strongly reduced to less than 12% in cortex and medulla of renal transplants with AR and ATN. F_P values correlated with creatinine clearance. *Conclusion:* DW-MRI allows reliable determination of diffusion and micro-circulation contributions in renal allografts shortly after transplantation; deviations in AR indicate potential clinical utility of this method to non-invasively monitor derangements in renal allografts.

Keywords Diffusion · Perfusion · Kidney · Acute rejection · Allograft · Transplantation

Introduction

Intense allograft monitoring and early characterisation of dysfunction after renal transplantation are important to allow initiation of appropriate treatment and to improve the rate of successful outcome. Among others, acute rejection (AR) remains a major complication after renal transplantation, which may reduce both short- and long-term graft survival [1]. Until now, no reliable and accurate non-invasive clinical methods were available to diagnose and distinguish between different renal allograft derangements such as AR and acute tubular necrosis (ATN).

Diffusion-weighted MR imaging (DW-MRI) is a promising non-invasive MR imaging method to obtain functional information about the renal allograft. Its application may therefore be instrumental in monitoring patients early after kidney transplantation. DW-MRI yields a total "apparent diffusion coefficient" (ADC_T) that provides information on diffusion properties, but also includes contributions from concurrent micro-circulation [2]. Provided diffusion and micro-circulation contributions can be separated, DW-MRI may in addition provide information on micro-circulation, quantified with the "perfusion fraction" (F_P), and "perfusion-free" diffusion (ADC_D).

Compared with the brain, in which DW-MRI is routinely performed, applications in abdominal organs are only currently evolving because of a number of technical challenges, including respiratory and cardiac motion as well as susceptibility artefacts [3–5]. Although DW-MRI has been successfully applied in a number of studies for functional characterisation of native kidneys (for an overview see [6]), to date only one animal study has examined transplanted kidneys with DW-MRI [7], and only one study in human transplanted kidneys has been published, demonstrating the feasibility and reproducibility of DW-MRI in allografts with stable function at least 4 months after transplantation [8]. In addition, the latter DW-MRI study was the first to separately analyse the micro-circulation contribution in stable human transplanted kidneys. No DW-MRI study has yet been performed in human renal allografts shortly after transplantation, neither in healthy nor diseased patients. Previous studies have suggested that complications in renal allografts, like acute rejection, may lead to altered blood flow and/or changes in reabsorption and concentration-dilution function [9, 10]. The separation of diffusion and micro-circulation contributions may therefore be especially interesting in this condition.

Almost all previously published DW-MRI measurements in kidneys were performed at the lower field strength of 1.5 T, while 3-T MRI is being introduced more and more into clinical routine, mostly because of higher sensitivity [5]. Previously, we showed that DW-MRI obtained on 1.5-T MRI in transplanted kidneys with good renal function about 9 months after transplantation yields stable and reproducible values for the total apparent diffusion coefficient (ADC_T), corresponding to the commonly determined diffusion parameter, the "perfusion-free" diffusion coefficient (ADC_D) and—although less stable—the micro-circulation contribution [8].

The main goals of the current DW-MRI study on 3-T MRI in renal allografts shortly after transplantation were to determine the inter-patient variability of diffusion parameters, including perfusion contributions, and to gain initial information on whether these measures are altered in histologically proven acute allograft rejection, providing a first impression of the sensitivity of the method.

Materials and methods

Patients and volunteers

The local ethics committee approved the study protocol and all participants provided written informed consent.

The study group comprised 15 renal transplant patients (10 men, 5 women; mean age 47±11 years; age range 31–65 years), 11 first, 2 second and 2 third transplantations (Table 1). All transplant recipients eligible for the study and providing written informed consent were included in the study over a total period of 7 months. Mean time between transplantation and MRI was 10±4 days (range 5–19 days). Delayed graft function occurred in four patients. Six patients received a kidney transplant biopsy which showed AR in four patients (two patients with signs of acute humoral rejection, positive C4d staining and presence of donor-specific serum antibodies, and two patients with acute cellular rejection), ATN/cholesterol embolism in one patient, and no AR or ATN, but signs of a donor-derived hyaline arteriolosclerosis in one patient. The last patient was considered to have a normal functioning transplant because no other clinical signs of allograft dysfunction were detected. In addition, 9 of the 15 patients demonstrated no clinical sign of major allograft complications and these patients were also considered to have a stable transplant function. Histological diagnosis was assessed according to the Banff criteria [11–13]. For those patients undergoing a biopsy, the MR examination was performed within 5 days of the biopsy. No other imaging modality for detection of graft rejection was performed.

The subjects were told to eat and drink moderately; however, exact control of their hydration status was unnecessary, because only a low impact on diffusion results under normal conditions was expected [6]. All patients received triple immunosuppressive therapy based on a combination of cyclosporine starting at day 1 post-operatively, mycophenolate mofetil or mycophenolic acid and prednisone. Induction therapy was applied with basiliximab (Simulect®) on day 0 and day 4 in all patients. One patient (S13) with a panel reactive antibody (PRA) of 63% at transplantation additionally received intravenous immunoglobulin therapy (Octagam® Octapharma, Lachen, Switzerland) from day 0 to 3 post-transplantation.

Anti-rejection therapy consisted of at least three intravenous methylprednisolone pulses in all patients with signs of AR, and additional plasmapheresis treatment for the two patients with acute humoral rejection.

Serum creatinine (s-Crea) concentrations were obtained from all subjects on the day of the MR examination and were used to calculate the creatinine clearance (eGFRc) using the Cockcroft–Gault formula [14].

Table 1 Patient characteristics

Subject	Sex	Recipient age (years)	Donor age (years)	Time period between Tx and MR (days)	No. Tx	DGF	Biopsy diagnosis/ remark	s-Crea at time of MR examination (μmol/l)	eGFRc at time of MR examination (ml/min/1.73 m^2)	eGFRc 1 year after Tx (ml/min/1.73 m^2)	Results of morphological MRI
S1	M	62	33	13	2	0	NA	92	83	80	Lymphocele
S2	M	34	22	10	2	0	NA	83	108	68	Normal for new (2nd) kidney
S3	M	35	43	7	1	0	NA	90	111	95	Small lymphocele
S4	F	31	40	5	3	0	NA	63	85	61	Normal
S5	F	33	44	19	1	0	NA	117	99	130	Normal
S6	M	53	55	9	1	0	NA	174	55	94	Cortical cyst upper pole
S7	M	38	72	7	1	0	Arteriolar hyalinosis	244	44	35	Normal
S8	M	48	22	8	1	0	NA	91	75	50	Normal
S9	M	65	69	12	1	1	NA	118	68	87	Cortical cyst upper pole
S10	M	40	26	7	1	0	NA	135	78	98	Normal
S11	M	41	61	6	1	1	ATN/cholesterol embolism	440	24	30	Highly abnormal with patchy hypointensities and absent cortico-medullary differentiation
S12	M	59	58	10	1	0	ACR	230	29	27	Reduced cortico-medullary differentiation
S13	F	61	53	15	3	0	AHR	102	52	80	Normal
S14	F	44	60	8	1	1	AHR	315	31	No #	Normal
S15	F	51	61	13	1	1	ACR	348	15	No (death)	Absent cortico-medullary differentiation

Abbreviations: *M* male, *F* female, *Tx* transplantation, *No.* number, *DGF* delayed graft function, *ACR* acute cellular rejection, *AHR* acute humoral rejection, *s-Crea* serum creatinine concentration, *eGFRc* estimated glomerular filtration rate calculated by Cockcroft–Gault formula, *NA* no biopsy available, # nephrectomy

After 1 year of clinical post-transplant follow-up, renal function was preserved in 13 patients, one kidney with a previous severe acute rejection episode had to be removed (S14), one patient died from an infectious complication unrelated to allograft function (S15). Follow-up examinations did not include DW-MRI.

MR investigations

The MR measurements were performed on a 3-T MRI system (TIM-Trio; Siemens, Erlangen, Germany) using a combination of a spine coil and a phased array body coil with six elements.

Before the patient investigations, the DW-MRI measurement parameters were optimised to achieve sufficient image quality, which is challenging in the abdomen, especially at higher field strengths. Optimisation included reduction of echo times and geometric distortions by selection of bandwidth or parallel imaging acceleration factor, or evaluation of the benefit using a dielectric pad to reduce signal voids from dielectric effects [15]. Morphological imaging included coronal T2-weighted half-Fourier acquisition single-shot turbo spin-echo (HASTE) imaging, and axial and coronal T1-weighted fast low angle shot (FLASH) gradient-echo imaging. For DW-MRI, a coronal diffusion-weighted multisection single-shot echo-planar imaging sequence was applied. In order to be able to separate micro-circulation from diffusion contributions, ten diffusion gradient b values between 0 and 700 s/mm^2 were applied (0, 10, 20, 50, 100, 180, 300, 420, 550, 700 s/mm^2). The maximum b value was chosen based on previously determined renal ADC values leaving sufficient signal clearly above noise level. The b values were spaced non-equidistantly with several low b values, to account for the fast-decaying contribution from micro-circulation.

The following imaging parameters were used: 11 slices with a thickness of 5 mm and an intersection gap of 1 mm, field of view = 400×400 mm^2, matrix = 128×128, six averages, bandwidth = 2,300 Hz/pixel, voxel size = 3.1×3.1×5.0 mm^3, phase encoding direction RL. The diffusion gradients were applied in three orthogonal directions and subsequently averaged, minimising effects of diffusion anisotropy. Parallel imaging (iPAT, GRAPPA) with an acceleration factor of 3 was applied. Respiratory triggering was used to reduce motion artefacts with a minimum TR of 2,800 ms and TE of 64 ms. Slice positioning was identical to the coronal T1-weighted sequence. Minimum acquisition time was 8 min, depending on the breathing cycle. The entire MR examination including positioning, morphological imaging and DW-MRI lasted about 30 min.

Image analysis

All participants' studies were included in the analysis. The data were evaluated on an independent workstation using a home-built IDL program (Interactive Data Language, RSI, Boulder, CO, USA).

Morphological evaluation

The morphological images were read by an experienced radiologist, subspecialised in urogenital radiology. The findings are summarised in Table 1.

DW-MRI evaluation

DW-MRI findings were analysed completely blinded with respect to all clinical findings to eliminate any bias. Processing of the DW-MRI data was performed on a pixel-by-pixel basis in two different ways as previously described [8]. In brief: (1) A single ADC value (ADC_T) was calculated from all b values using a monoexponential fitting model and includes contributions from both diffusion and perfusion. This method corresponds to the commonly applied procedure. (2) In a second analysis of the same data, diffusion and micro-circulation contributions were separated by biexponential fitting (assuming a fast- and slow-decaying component with increasing b values assigned to perfusion and diffusion contributions, respectively) of the signal intensities at all multiple b values. This analysis yielded (a) the "perfusion fraction" (F_P), i.e. the contribution of micro-circulation of blood and movement in predefined structures such as renal tubules, and (b) an ADC value (ADC_D), reflecting predominantly pure diffusion. From the results for each pixel, maps for the different diffusion parameters were created and could be displayed.

Ellipsoid regions of interest (ROIs) were positioned on coronal T1-weighted images for anatomical guidance and simultaneously on co-registered diffusion images at b=0 s/mm^2 or on calculated diffusion maps. The ROIs were placed in the upper, mid and lower poles of the cortex and medulla on several slices covering large parts of the allograft (mean total number of ROIs 11.0±3.8 for both cortex and medulla; mean individual ROI size 0.47±0.02 cm^3 and 0.45±0.02 cm^3 for cortex and medulla, respectively). Single total ROIs were created separately for cortex and medulla by merging all individual ROIs, yielding one ROI for the cortex and one for the medulla. This procedure yields overall cortical or medullary diffusion properties. However, in order to assess possible focal changes in addition, which might be missed or diluted otherwise, an individual ROI

was placed in a "selected region" for each subject, i.e. in a hypo- or hyperintense region within renal tissue on the diffusion maps. This was performed no matter if this region appeared to be within normal range or not. As all processing steps, including diffusion map inspection and ROI positioning, were performed blinded to the results no bias was introduced by examining "selected regions".

Statistical analysis

For this initial study, which aims to determine the feasibility of performing DW-MRI measurements in renal allografts early after transplantation, a sample size of ten patients with stable allograft function and of another five patients with complications was considered sufficient. A power analysis based on these numbers and on previous DW-MRI results [8] yields a difference between deranged and stable kidneys of less than 10% in ADC_D and ADC_T and of approximately 40% in F_P which could be detected at a significance level of 0.05 and a statistical power of 80%. These calculated differences can be presumed reasonable in view of previous results. However, a detailed quantitative comparison between the groups was beyond the scope of the present investigation.

Mean and standard deviations of ADC_T, ADC_D and F_P were calculated for the ten patients without clinical or laboratory signs of transplant dysfunction and paired *t* tests were performed for group comparisons between cortex and medulla in stable allografts after testing for normal distribution with a Kolmogorov–Smirnov Test. The Mann–Whitney *U* test for unpaired samples was performed for comparisons between stable allografts and kidneys with acute rejection. However, because of the low number of patients with transplant dysfunction, the results were compared mainly descriptively as an indication of a possible trend for differences between the groups. Diffusion parameters were correlated with the estimated creatinine clearance by employing Pearson linear regression analysis. A p value of less than 0.05 was considered statistically significant. Statistical analysis was performed with SPSS, version 12.0.1 (SPSS Inc., Chicago, Ill, USA).

Results

Stability of parameters from DW-MRI

No patient data had to be removed from the analysis because of insufficient quality, i.e. all 15 investigated subjects were included in the analysis. Mean values and standard deviations of ADC_T, ADC_D and F_P values in medulla, cortex and in selected regions were calculated from the ten patients with stable allograft function (Table 2). Standard deviations for all ADC values were low with coefficients of variation in the range of 4–7%, while for F_P the variance was greater with approximately 25%. ADC_T and F_P values were similar in cortex and medulla. On the other hand, ADC_D values were slightly, but significantly, higher in cortex than in medulla (203 ± 9 vs. $199\pm9\times10^{-5}$ mm^2/s, $p<0.02$).

Diffusion maps: examples and comparison with histology

In two subjects (S1, S2) with second transplantation, but stable allograft function, the DW-MRI measurement covered both the recently transplanted functioning kidney as well as the previously transplanted non-functioning kidney within the same image planes. This allows for an illustrative comparison of maps of the derived parameters between the two kidneys (Fig. 1 shows the maps of S2) and may provide a first impression of the sensitivity of this method. The parameters ADC_T, ADC_D and especially the perfusion fraction F_p were strongly reduced in the older and insufficiently functioning kidneys compared with the new allografts (Fig. 1). The overall values for the two older allografts were $ADC_T=165$ and 169×10^{-5} mm^2/s, $ADC_D=157$ and 153×10^{-5} mm^2/s, $F_P=6$ and 11%, for S1 and S2, respectively.

DW-MRI parameter maps of an allograft with acute rejection (see Table 1, patient S14) are shown in Fig. 2 together with the corresponding histological sections from the transplant biopsy. The strongly reduced ADC_T, ADC_D and F_P in this subject (see Table 2) may correspond to interstitial leukocytic infiltration, peritubular capillaritis and/or tubular casts as shown on the histological section (see Fig. 2).

Results from DW-MRI in kidneys with relevant functional derangements

The ADC_T values of the four grafts with histologically proven evidence of acute rejection were lower than those of eight (cortex and medulla) or nine (selected regions) of the ten recipients with stable allograft function (Table 2). The ADC_T differences between the two patient groups were significant for all tissue types ($p<0.03$).

Compared with ADC_T, ADC_D values, which mostly represent pure diffusion, were relatively similar for all subjects (Table 2). It is interesting to note that the only kidney that had to be nephrectomised 50 days after the MR measurement because of persistent acute humoral rejection had by far the lowest ADC_T and ADC_D values in all the regions investigated (S14 in Table 2). Remarkably,

Table 2 Results from DW-MRI in renal allografts with and without functional derangements

Diagnosis	Subject	Cortex			Medulla			Selected region[a]		
		ADC_T (10^{-5} mm^2 /s)	ADC_D	F_P (%)	ADC_T (10^{-5} mm^2 /s)	ADC_D	F_P (%)	ADC_T (10^{-5} mm^2 /s)	ADC_D	F_P (%)
Stable renal function	S1	217	209	8	209	197	10	218	203	12
	S2	240	207	23	246	204	27	241	204	24
	S3	230	204	19	225	196	20	221	199	17
	S4	200	183	12	194	180	10	192	175	13
	S5	225	199	18	216	192	17	218	194	17
	S6	246	211	25	241	208	24	240	210	21
	S7	233	204	19	240	204	22	233	207	19
	S8	240	214	19	234	203	21	221	193	20
	S9	220	193	18	221	193	18	218	189	20
	S10	234	209	18	234	210	18	235	208	19
	Mean ± sd	228±14	203±9	18±5	226±16	199±9	19±5	224±15	198±11	18±4
ATN	S11	209	198	8	215	203	9	211	206	6
Acute rejection	S12	217	205	9	197	183	10	195	180	11
	S13	205	193	10	203	192	9	198	189	9
	S14	161	145	11	171	154	12	160	142	13
	S15	219	206	11	212	199	10	214	209	6

Mean and standard deviation (sd) were calculated for allografts with normal function.
[a]A hypo- or hyperintense region on the diffusion maps (selected blinded to the results) that revealed deviations from normal appearance

allografts with an acute rejection demonstrated reduced micro-circulation contributions in medulla ($p<0.03$), cortex ($p<0.03$) and in selected regions in the allograft ($p<0.01$): F_P values were lower in all four rejecting kidneys than in 9/10 (cortex) and in 8/10 (medulla and selected regions) kidneys with stable function (Fig. 3).

ADC_T in the single patient with ATN and additional signs of cholesterol emboli appeared slightly decreased

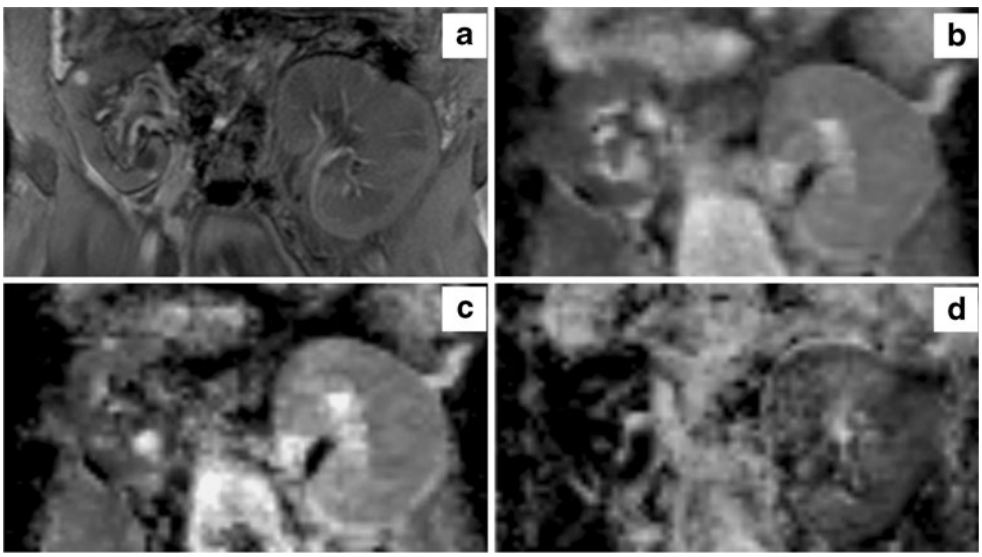

Fig. 1 Morphological MR images and parameter maps from DW-MRI of one subject (S2) presenting first with an inadequately functioning allograft (right side) and a well-functioning allograft (left side). T1-weighted FLASH-MRI (**a**), maps for ADC_T (**b**), ADC_D (**c**) and F_P (**d**). The signal intensity was lower (*darker shade*) on all diffusion maps of the first implanted (smaller) kidney compared with the recently implanted kidney. The difference between the first and the second allograft appears to be most pronounced for F_P and to a lesser extent for ADC_D and ADC_T. A small haemorrhagic cyst in the upper pole and a small simple cyst in the lower pole of the right kidney are visualised

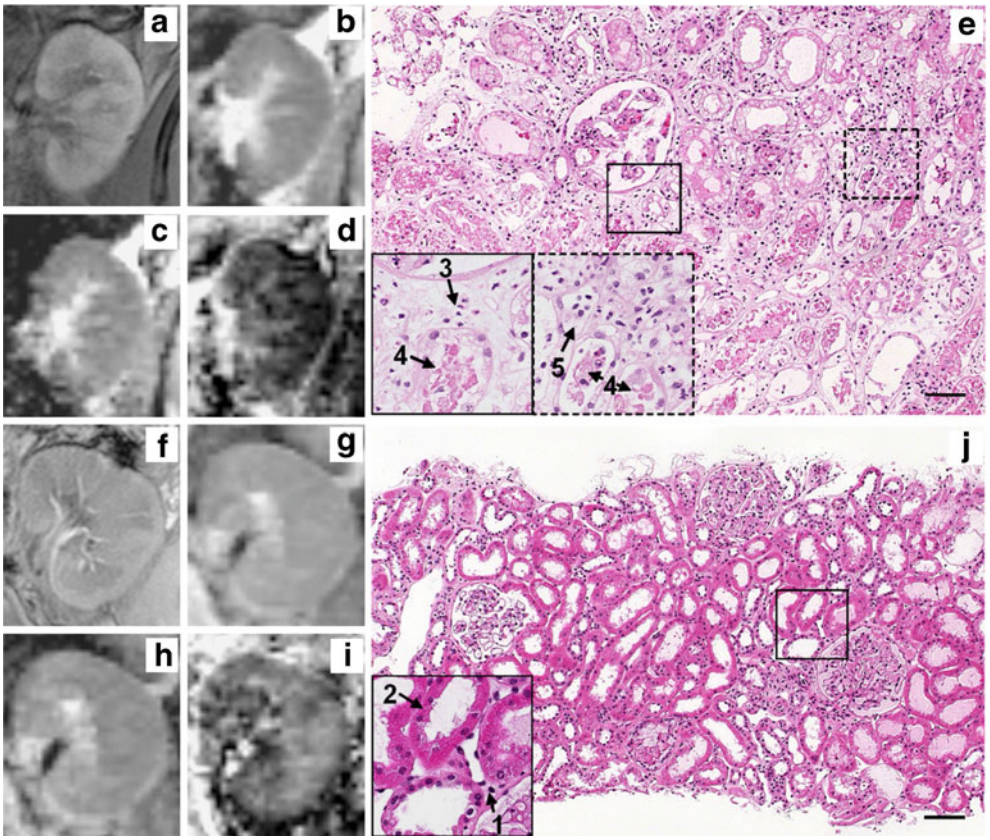

Fig. 2 Morphological MRIs (**a**), maps for ADC_T (**b**), ADC_D (**c**), F_P (**d**) and corresponding histological section (**e**) for S14 presenting with signs of acute humoral rejection, namely interstitial oedema and peritubular capillaritis (*5*), as well as a low-grade interstitial infiltrate (*3*). The morphological MR images did not show any conspicuities. For comparison, corresponding MRIs (**f**–**i**) of a well-functioning kidney and a normal histological section (**j**) are also presented. The *arrows* pinpoint *1* = interstitial space, *2* = proximal tubule, *3* = interstitial leukocytic infiltration, *4* = tubular cast, *5* = peritubular capillaritis (H&E staining, *bar* = 100 μm)

and, in particular, the micro-circulation contribution F_P was very low in all tissues investigated (Table 2 and Fig. 3).

Comparison between parameters from DW-MRI and estimated glomerular filtration rate calculated with the Cockcroft–Gault formula (eGFRc)

Significant correlations were determined between eGFRc and the micro-circulation contribution (F_P) in cortex (R=0.53, p<0.05, Fig. 4a), medulla (R=0.52, p<0.05, Fig. 4b) and selected regions (R=0.63, p<0.02, Fig. 4c). Estimated GFRc did not correlate significantly with ADC_T or ADC_D in any of the renal regions investigated.

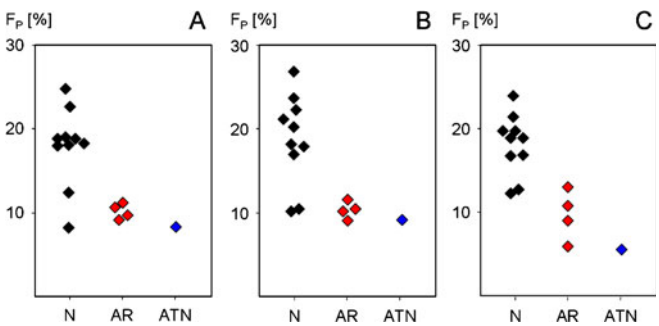

Fig. 3 Perfusion fraction, F_P (%), in cortex (**a**), medulla (**b**) and "selected regions" (**c**) for transplanted kidneys with normal function (*N*), acute rejection (*AR*) or acute tubular necrosis (*ATN*)

Discussion

The results of this DW-MRI study on 3-T MRI demonstrate that diffusion parameters can be determined in well-functioning renal allografts shortly after transplantation with low inter-patient variability, also including determination of micro-circulation contributions; the magnitude of changes of the parameters assessed in subjects with histologically proven acute rejection or ATN indicates potential clinical utility of the method to non-invasively monitor derangements in renal allografts.

Other non-invasive methods of detecting allograft dysfunction

Many diagnostic attempts have been made to reduce the need for an invasive transplant biopsy, considered the "gold standard" for the diagnosis of parenchymal dysfunction, including acute rejection. Ultrasound characteristics of rejection occur only late after rejection and are non-specific [16]. The addition of serial measurements of resistance index by colour-coded duplex ultrasound

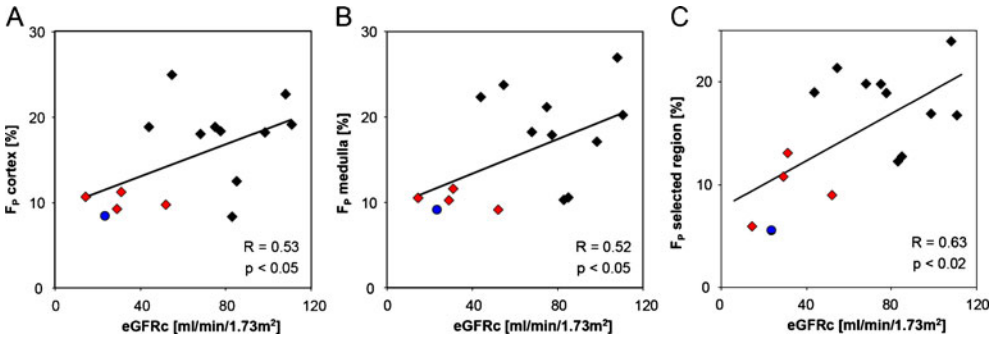

Fig. 4 Correlation between estimated glomerular filtration rate (eGFRc) calculated by the Cockcroft–Gault formula and F_P (%) in cortex (**a**), medulla (**b**) and selected regions (**c**). *Black diamonds* normal function, *red diamonds* acute rejection, *blue circle* ATN

increases the sensitivity, but specificity remains low [17, 18]. The diagnostic value of renal scintigraphy, especially for prediction of acute rejection, is also limited [19].

The most consistent sign of acute rejection reported is the loss of cortico-medullary differentiation on contrast-enhanced MR renography [20], although it appears to be a relatively non-specific finding in acute rejection, with overlap with other disease processes [21]. Thus, other non-invasive methods have to be considered, including MR-based functional renal imaging.

Blood oxygen level-dependent (BOLD) MRI has been shown to be of potential clinical value in transplanted kidneys [8] and may be helpful for evaluation and separation of kidney allograft dysfunction like ATN or acute rejection [22, 23]. Previously we have shown that the relaxation rate from BOLD MRI and F_P from DW-MRI provide complementary information [8]. Accordingly, a comparison of the two methods in renal dysfunction would be of interest. However, BOLD MRI in renal transplantation appears more challenging at 3 T than 1.5 T and is prone to artefacts, presently limiting its utility [24].

Stability of parameters from DW-MRI and diffusion and perfusion separation

A separation of diffusion and perfusion contributions from DW-MRI measurements was accomplished in the present study, yielding ADC_D, which reflects primarily pure diffusion, and F_P, the perfusion fraction, which reflects micro-circulation of blood and/or movement of fluids in predefined structures such as tubules and glomeruli. ADC values and F_P, although less marked, exhibited a low inter-subject variability in the 10 stable functioning allografts early after transplantation.

The separation of perfusion and diffusion parameters from DW-MRI measurements was first proposed about 20 years ago by Le Bihan et al. [2] and has been discussed ever since, also for imaging of abdominal organs [25–28]. The current investigation suggests that this separation may be clinically useful and provides additional information compared with the standard procedure of estimating only a single ADC value, corresponding to ADC_T in our analysis. This separation may lead to a better differentiation between different entities, as suggested in the present study when the distinct parameters were compared between stable and acutely rejected kidneys. Although speculative on the basis of only four cases of rejection, the lower F_P in grafts with AR in the presence of relatively unchanged ADC_D suggests that lower micro-circulation rather than reduced diffusion accounts for the lower ADC_T. A similar finding was observed recently in a DW-MRI study by Luciani et al. [26] in patients with liver cirrhosis: While ADC_D values appeared unchanged, indicating unchanged diffusion, the perfusion was decreased in cirrhotic patients. Without the diffusion/perfusion separation, these changes would have been missed, or erroneously attributed to altered diffusion.

In the current study, mean values and standard deviations for ADC_D and F_P in patients with stable allograft function 10±4 days after transplantation are very similar to those of our previous investigation in 15 stable renal allografts on average 9 months after transplantation, despite differences in measurement parameters and field strength [8] (previously, ADC_D values ($\times 10^{-5}$ mm^2/s) were 198±10 and 198±7 in cortex and medulla, respectively; F_P values were 19±4% and 18±5% in cortex and medulla, respectively). The ADC_T values were slightly higher in the allografts of the current study compared with the previous ones (previously, ADC_T values ($\times 10^{-5}$ mm^2/s) were 217±14 and 217±11 in cortex and medulla, respectively). In line with the present results, ADC_T and F_P were previously found to be similar in cortex and medulla of transplanted kidneys, a finding contrary to that of native kidneys with higher ADC and F_P values in cortex than in medulla [8]. In our previous study, ADC_D values determined in renal allografts were also not different in medulla and cortex. In the present investigation, however, ADC_D values were slightly higher in the cortex compared with the medulla. This may be a spurious difference or may be due to the different time point of the measurements after transplantation. Nevertheless, the similarity between the previously and currently determined values, obtained on various imaging systems with different measurement parameters and field strengths, suggests that the results may be comparable in absolute terms across different studies or institutions. However, the separation of micro-circulation contributions and diffusion appears to be a prerequisite. If this separation is neglected, the resulting ADC values will

depend on the measurement parameters, namely the strength of parameters for diffusion weighting. This most likely explains the anticipated differences between the ADC_T values in the previous and current studies. Similarly, different diffusion-weighting parameters probably account for inconsistencies and differences between published "total" ADC values for native kidneys (for an overview see e.g. [6, 29]).

Functional relevance and limitations of the study

The micro-perfusion contribution was lower in cortex, medulla and "selected regions" of the four kidney transplants with evidence of rejection compared with stable transplants. The changes in AR were only slightly more pronounced in "selected regions" (Fig. 3). Thus, compared to overall cortical or medullary diffusion properties the analysis of "selected regions" did not yield a clearly superior separation of the few allografts with dysfunction. Nevertheless, in combination with simple determination of signal intensities of the diffusion maps the rather strong ADC_T and F_P reductions in dysfunction may suggest a clinical role for visual analysis of individual diffusion maps.

The decreased F_P paralleled a reduced estimated GFR. These results are in line with observations by Jani et al. [10], who quantified renal blood flow by *para*-aminohippuric acid and GFR by inulin clearance in patients with acute rejection and observed a decrease in renal blood flow by 45 to 70% and a reduced GFR. Besides the rejection process, the impaired haemodynamics might partly be explained by the administration of calcineurin inhibitors [30]. However, since the immunosuppressive regime in all our study patients was the same and calcineurin levels comparable (results not shown), it is unlikely that calcineurin inhibition accounts for the differences in micro-circulation observed between patients with and without functional derangements [31, 32]. Thus, according to our preliminary results, F_P may help to estimate changes in renal blood flow non-invasively in different parts of the kidney and provide further insight into mechanisms accounting for impaired renal haemodynamics after renal transplantation.

There are a number of limitations to our study: First, although care was taken not to select regions for determining diffusion parameters in the kidneys that were close to the site of biopsy, it cannot be excluded that the biopsy, which was performed mostly in patients with acute rejection, may have affected the results. Second, the patients with rejection had already been given a high dose of methylprednisolone at the time of the MR investigation. Although unlikely, we cannot exclude an effect of this intervention independent of the histologically proven rejection. Third, ROI placement and reading was performed by only one reader and only once, potentially introducing reader related bias and preventing determination of inter- and intra-rater reliability. Forth, the clinical utility of the time-consuming and costly MR investigation awaits confirmation in a larger cohort and no final conclusion on its value in AR can currently be drawn. This is especially true for the single ATN case: although the finding of reduced micro-circulation is reasonable in a physiological sense, it is not possible to draw any clinically relevant conclusion on whether the method allows AR to be distinguished from ATN.

Conclusion

The application of DW-MRI in renal allografts holds promise as a tool for non-invasive detection and monitoring of functional and structural derangements early after transplantation.

Acknowledgement This work was supported by the Swiss National Foundation 320000–113512/1 and 320000–111959/1.

References

1. Cecka JM (2003) The OPTN/UNOS renal transplant registry 2003. Clin Transpl 1–12
2. Le Bihan D, Breton E, Lallemand D, Aubin ML, Vignaud J, Laval-Jeantet M (1988) Separation of diffusion and perfusion in intravoxel incoherent motion MR imaging. Radiology 168:497–505
3. Prasad PV, Priatna A (1999) Functional imaging of the kidneys with fast MRI techniques. Eur J Radiol 29:133–148
4. Schick F (2005) Whole-body MRI at high field: technical limits and clinical potential. Eur Radiol 15:946–959
5. Machann J, Schlemmer HP, Schick F (2008) Technical challenges and opportunities of whole-body magnetic resonance imaging at 3T. Phys Med 24:63–70
6. Thoeny HC, De Keyzer F, Oyen RH, Peeters RR (2005) Diffusion-weighted MR imaging of kidneys in healthy volunteers and patients with parenchymal diseases: initial experience. Radiology 235:911–917
7. Yang D, Ye Q, Williams DS, Hitchens TK, Ho C (2004) Normal and transplanted rat kidneys: diffusion MR imaging at 7 T. Radiology 231:702–709
8. Thoeny HC, Zumstein D, Simon-Zoula S, Eisenberger U, De Keyzer F, Hofmann L, Vock P, Boesch C, Frey FJ, Vermathen P (2006) Functional evaluation of transplanted kidneys with diffusion-weighted and BOLD MR imaging: initial experience. Radiology 241:812–821

9. Venz S, Kahl A, Hierholzer J, Gutberlet M, Windrich B, Bechstein WO, Hosten N, Frei U, Felix R (1999) Contribution of color and power Doppler sonography to the differential diagnosis of acute and chronic rejection, and tacrolimus nephrotoxicity in renal allografts. Transpl Int 12:127–134
10. Jani A, Polhemus C, Corrigan G, Kwon O, Myers BD, Pavlakis M (2002) Determinants of hypofiltration during acute renal allograft rejection. J Am Soc Nephrol 13:773–778
11. Racusen LC, Solez K, Colvin RB, Bonsib SM, Castro MC, Cavallo T, Croker BP, Demetris AJ, Drachenberg CB, Fogo AB, Furness P, Gaber LW, Gibson IW, Glotz D, Goldberg JC, Grande J, Halloran PF, Hansen HE, Hartley B, Hayry PJ, Hill CM, Hoffman EO, Hunsicker LG, Lindblad AS, Yamaguchi Y (1999) The Banff 97 working classification of renal allograft pathology. Kidney Int 55:713–723
12. Racusen LC, Colvin RB, Solez K, Mihatsch MJ, Halloran PF, Campbell PM, Cecka MJ, Cosyns JP, Demetris AJ, Fishbein MC, Fogo A, Furness P, Gibson IW, Glotz D, Hayry P, Hunsickern L, Kashgarian M, Kerman R, Magil AJ, Montgomery R, Morozumi K, Nickeleit V, Randhawa P, Regele H, Seron D, Seshan S, Sund S, Trpkov K (2003) Antibody-mediated rejection criteria-an addition to the Banff 97 classification of renal allograft rejection. Am J Transplant 3:708–714
13. Solez K, Colvin RB, Racusen LC, Haas M, Sis B, Mengel M, Halloran PF, Baldwin W, Banfi G, Collins AB, Cosio F, David DS, Drachenberg C, Einecke G, Fogo AB, Gibson IW, Glotz D, Iskandar SS, Kraus E, Lerut E, Mannon RB, Mihatsch M, Nankivell BJ, Nickeleit V, Papadimitriou JC, Randhawa P, Regele H, Renaudin K, Roberts I, Seron D, Smith RN, Valente M (2008) Banff 07 classification of renal allograft pathology: updates and future directions. Am J Transplant 8:753–760
14. Cockcroft DW, Gault MH (1976) Prediction of creatinine clearance from serum creatinine. Nephron 16:31–41
15. Vermathen P, Eisenberger U, Boesch C, Thoeny HC (2006) Diffusion weighted imaging in native and transplanted human kidneys at 3T. Initial experience. Proc Intl Soc Magn Reson Med 14:1234
16. Baxter GM (2001) Ultrasound of renal transplantation. Clin Radiol 56:802–818
17. Hollenbeck M, Hilbert N, Meusel F, Grabensee B (1994) Increasing sensitivity and specificity of Doppler sonographic detection of renal transplant rejection with serial investigation technique. Clin Investig 72:609–615
18. Tublin ME, Bude RO, Platt JF (2003) Review. The resistive index in renal Doppler sonography: where do we stand? AJR Am J Roentgenol 180:885–892
19. Heaf JG, Iversen J (2000) Uses and limitations of renal scintigraphy in renal transplantation monitoring. Eur J Nucl Med 27:871–879
20. Hricak H, Terrier F, Marotti M, Engelstad BL, Filly RA, Vincenti F, Duca RM, Bretan PN Jr, Higgins CB, Feduska N (1987) Posttransplant renal rejection: comparison of quantitative scintigraphy, US, and MR imaging. Radiology 162:685–688
21. Zhang H, Prince MR (2004) Renal MR angiography. Magn Reson Imaging Clin N Am 12:487–503 vi
22. Sadowski EA, Fain SB, Alford SK, Korosec FR, Fine J, Muehrer R, Djamali A, Hofmann RM, Becker BN, Grist TM (2005) Assessment of acute renal transplant rejection with blood oxygen level-dependent MR imaging: initial experience. Radiology 236:911–919
23. Djamali A, Sadowski EA, Samaniego-Picota M, Fain SB, Muehrer RJ, Alford SK, Grist TM, Becker BN (2006) Noninvasive assessment of early kidney allograft dysfunction by blood oxygen level-dependent magnetic resonance imaging. Transplantation 82:621–628
24. Agrawal G, Fain SB, Artz N, Wentland AL, Grist TM, Djamali A, Sadowski EA (2009) Blood-oxygen level dependent (BOLD) imaging in native and transplanted kidneys on 1.5T and 3.0T. Proc Intl Soc Magn Reson Med 17:2027
25. Muller MF, Prasad PV, Edelman RR (1998) Can the IVIM model be used for renal perfusion imaging? Eur J Radiol 26:297–303
26. Luciani A, Vignaud A, Cavet M, Nhieu JT, Mallat A, Ruel L, Laurent A, Deux JF, Brugieres P, Rahmouni A (2008) Liver cirrhosis: intravoxel incoherent motion MR imaging-pilot study. Radiology 249:891–899
27. Le Bihan D (2008) Intravoxel incoherent motion perfusion MR imaging: a wake-up call. Radiology 249:748–752
28. Wirestam R, Borg M, Brockstedt S, Lindgren A, Holtas S, Stahlberg F (2001) Perfusion-related parameters in intravoxel incoherent motion MR imaging compared with CBV and CBF measured by dynamic susceptibility-contrast MR technique. Acta Radiol 42:123–128
29. Thoeny HC, De Keyzer F (2007) Extracranial applications of diffusion-weighted magnetic resonance imaging. Eur Radiol 17:1385–1393
30. Myers BD, Newton L (1991) Cyclosporine-induced chronic nephropathy: an obliterative microvascular renal injury. J Am Soc Nephrol 2:S45–S52
31. Nilsson L, Ekberg H, Falt K, Lofberg H, Sterner G (1994) Renal arteriovenous shunting in rejecting allograft, hydronephrosis, or haemorrhagic hypotension in the rat. Nephrol Dial Transplant 9:1634–1639
32. Tinckam KJ, Djurdjev O, Magil AB (2005) Glomerular monocytes predict worse outcomes after acute renal allograft rejection independent of C4d status. Kidney Int 68:1866–1874